Journal of New Technology and Materials
JNTM
Vol. 01, N°00 (2011) 24-28

OEB Univ. Publish. Co.

Low Copper Doped CdO Nanowires Grown by Sol-Gel Route

M. Benhaliliba[a*], C.E. Benouis[a*], A. Tiburcio Silver[b]
[a] *Physics Department, Sciences Faulty, Oran University of Sciences and Technology USTOMB, BP1505 Oran, Algeria.*
[b]*ITT-DIEE, Apdo, Postal 20, Metepec 3, 52176, Estado de Mexico, Mexico.*
*Corresponding author bmost_31@yahoo.fr, Tel. +213772211491
Received: 23 May 2011, accepted: 30 September 2011

Abstract
In the current work, pure and copper doped cadmium oxide ($Cd_{1-x}Cu_xO$, x=0, 0.02, 0.03) thin films are grown by sol-gel spin coating route. Optical transmittance is measured in UV, VIS and IR spectra; it is revealed that the copper improves the transmittance. The optical band gap increased with the doping. The room temperature electrical resistance was affected by copper doping. The AFM morphology reveals that pure CdO and Cu doped thin films are nanostructured.
Keywords: *Sol-gel spin coating, Grain size, CdO, Cu level doping, Nanowires, Optical properties, AFM investigation.*

1. Introduction

Currently, Cadmium oxide (CdO) is among of interesting conducting oxide (TCO) group such as tin oxide (SnO_2) [1], indium oxide (In_2O_3) [2], indium tin oxide (ITO) [3] and zinc oxide ZnO [4-5] due to its high electrical and optical properties. Cadmium oxide (CdO) is n type semiconductor with direct band gap found to be 2.3 eV and it exhibits a cubic system and the lattice parameter is 4.695 Å [6]. Thin-film deposition techniques are either purely physical, such as evaporative methods, or simply chemical, such as gas and liquid phase chemical processes like sol-gel [7]. Furthermore, CdO has been deposited also by chemical bath (CBD) [8], spray pyrolysis [9], sputtering [10] and thermal evaporation [11]. Cadmium oxide is one of the promising II-VI family of semiconductors which has a great potential for optoelectronic devices [12]. CdO was doped with many elements such as Li [13], Al [14], Fe [15], Ga [16], Sm [17] and Eu [18, 19]. Up to our knowledge, there is no works published on the preparation and structural, UV-VIS-IR optical, AFM morphological and electrical properties investigation of Cu doped CdO. Our work consists on the preparation and characterization of CdO doped with transition metal (Cu), in the proportion 2 % and 3 %, to stand up their characterization for the advanced technological applications. The influence of Cu doping level on structural, optical, morphological, electrical properties of CdO synthesized by facile sol-gel spin coating route is investigated.

2. Experimental procedure

2.1. Films preparation

route onto microscope glass slides (76 x 26) mm^2 supplied by object trager Isolab. 0.5 Molar of cadmium acetate dihydrate ($Cd(CH_3COO)_2.2(H_2O)$) (purity of 99 %) supplied by Himedia, was dissolved in 10 ml of 2-Methoxyethanol ($C_3H_8O_2$) stirred at 60°C for 10 mn. The doping precursor was copper (II) acetate anhydrous $Cu(CH_3COO)_2$, (purity of 98 %) supplied by Carlo Erba reagents and then 0.3 ml of the Mono-Ethanolamine (MEA) C_2H_7NO (of molar mass 61.08 g/mol and density = 1.015) as stabilizer, was added drop by drop until the homogeneous and clear solution was obtained, then the stirring continued for 1hour. Consequently, the solution was aged for 24 hours until the gel formation at ambient (see scheme 1 and 2 [20]).

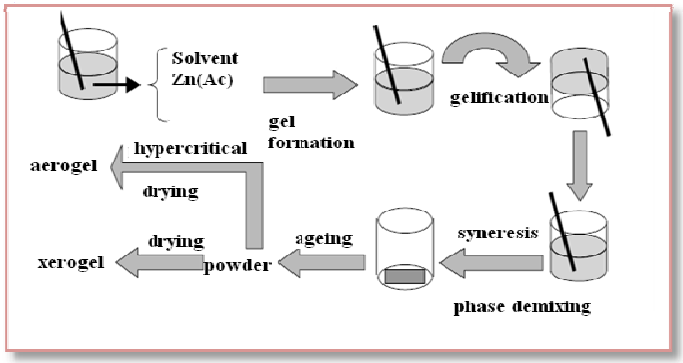

Scheme 1. Different steps of sol-gel process. (Aerogel is a manufactured material with the lowest bulk density of any known porous solid. It is derived from a gel in which the liquid component of the gel has been replaced with a gas), (Xerogel is a solid formed from a gel by drying with unhindered shrinkage. Xerogel is usually retain high porosity (25%) and enormous surface area (150–900 m^2/g), along with very small pore size 1-10 nm)[20].

Scheme 2. Sol-gel processing and ageing steps, resin formation

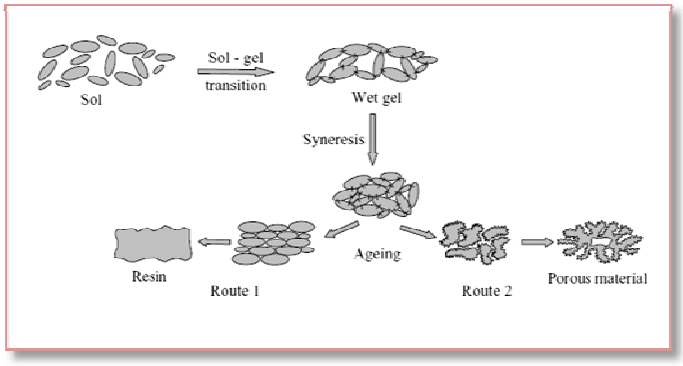

(route1) and porous solid material formation (route 2) [20].

The viscous solution was homogenously poured using micropipette on the substrate sticked on stainless steel spin plates of MTI, EQ-TC-100 Desk-top Spin Coater. The sample

rotates for one minute at speed of 1200 rotates per minute (RPM), the sample was heated at 150 °C for 10 mn and then the process was repeated 5 times, finally the film was annealed at 400 °C for 1hour under air in furnace MF 120 Nuve.

2.2. Films characterization

X-rays pattern of samples were carried out in Bruker AXS D8 Discover diffractometer, $CuK_{\alpha 1}$ (λ = 1.5418 A°) is used. The films coated transmittance and reflectance were recorded by Shimadzu 3600 PC double beam UV-VIS-NIR spectrometer, the electrical resistance at room temperature was then determined by four probes method. AFM observations of the coated films were made by using a Quesant Model 250 system having an 80x80 micrometer head, in the wave mode in air. For the (10 x10) micrometer square images the resolution was (300 x 300) pixels, the scan rate was 2 Hz for all cases. All analyses were performed with the software from the WSXM system

3. Results and discussion

3.1. Structural analysis

The figure 1A shows the X- rays diffraction pattern of pure and copper doped cadmium oxide where the angle ranges within 20°-80°. The grain size G is given by the well-known Scherrer's formula (1)[4],

$$G = \frac{0.94\ \lambda}{\beta\ \cos\ \theta} \quad (1)$$

Where β is the full width at half medium of the peak, 2θ is the Bragg angle and λ is X- rays wavelength. The calculated values of G are listed in table1.

Table1: Some parameters are calculated for pure and copper doped CdO

Sample	Grain size (nm)			TC (111)	E_g (eV)			T (550 nm) (%)
	(111)	(200)	(220)		$(\alpha h\nu)^2$	dT/dλ	dR/dλ	
CdO	8.235	8.245	6.199	1.80	2.49	2.59	2.52	56
CdO: Cu 2%	11.246	9.662	7.471	1.72	2.50	2.59	2.59	68
CdO: Cu 3%	8.801	7.853	7.122	1.73	2.56	2.62	2.59	79

The comparison of the observed XRD patterns with the standard JCPDS data (05-0640) confirms the structure of CdO phase with face centered cubic crystal structure [21]. The X rays pattern reveals that all investigated coated films are polycrystalline of cubic CdO structure and Bragg position for strong reflections like (111) direction was 32.92°, 33.08° and 33.09° respectively for pure and doped (2 % and 3 %) CdO coated films, and then a slight angle shift, estimated at 0.03°-0.16°, was carefully detected as sketched in fig. 1B. Others reflection positions (2θ) and their angle shifts are listed in table2.

Table1: X-rays results of pure and copper doped CdO

(hkl)		Bragg angle 2θ (°)	Angle shift Δ(2θ) (°)
(111)	CdO	32.92	-
	2%Cu	32.95	0.03
	3%Cu	33.08	0.16
(200)	CdO	38.12	-
	2%Cu	38.26	0.14
	3%Cu	38.43	0.31
(220)	CdO	55.06	-
	2%Cu	55.13	0.07
	3%Cu	55.30	0.24
(311)	CdO	65.70	-
	2%Cu	66.25	0.55
	3%Cu	66.42	0.72

These results are in well agreement with those of literature [22]. It seems that the CdO coated films have a preferential growth along the (111) direction. Most important peaks of CdO phase (111), (200), (220), (311) and (222) are shown in figure 1A. Textural coefficient is given by TC = I_{111}/ (1/4) (I_{111}+I_{200}+ I_{220}+I_{311}) [4] and data are tabulated according to (111) direction. The discrepancy in TC parameter is very low which confirms the crystalline structure is maintained at low doping level. Consequently, according to both (111), (220) orientations, copper doping increases the grain size, while 3 % copper level doping reduces it. As shown in figure 1B, CdO is present in coated film as confirmed by JCPDS card No. 05-0640, while a slight (2θ) shift to higher angle is caused by Cu doping. The ionic radii of Cu (II) and Cd (II) are respectively 0.73 Å and 0.95 Å and ionic radius ratio is $r_{Cu\ (II)}$/ $r_{Cd\ (II)}$=0.77, then cooper has minor radius than cadmium, it may diffuse in host lattice without causing mismatch or distortion, this fact corroborates with the slight angle shift. Figure 2 illustrates grain size of samples grown by spin coating route according to (111), (200) and (220) orientations. The grain size sweeps in average of 6 nm, these values due to X rays peaks broadening are minor; this confirms the nanostructures aspect of our coated films. Furthermore grain size is increased by the Cu doping level (2 %).

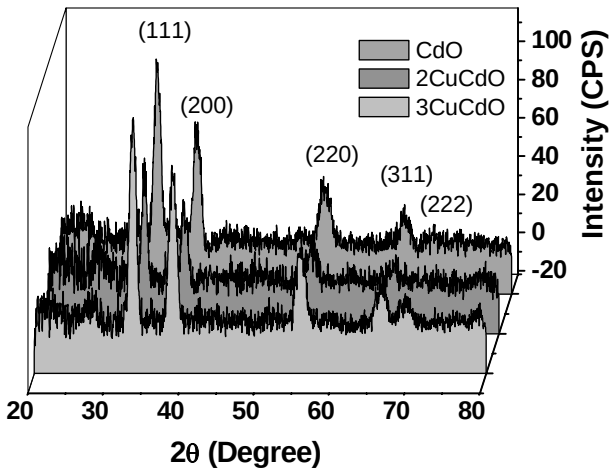

Figure 1A. X-rays pattern of pure and copper doped CdO grown by spin coating process at 1200 RPM, Bragg angle ranges within 20°-80°.

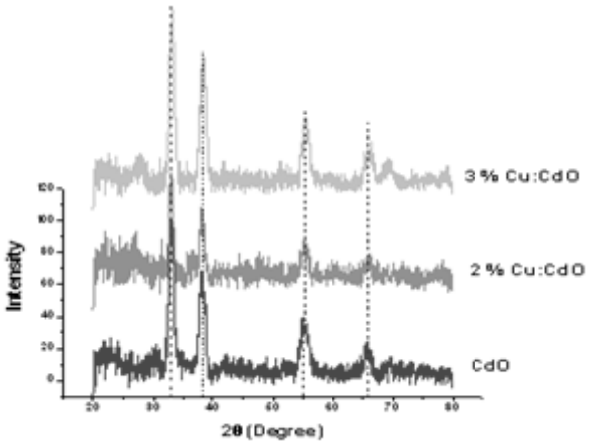

Figure 1B. JCPDS card No 05-0640 of pure and copper doped CdO are sketched (red dash lines). Slight angle shift (2θ) to higher angle is observed.

1.1. Optical characterization

The transmittance of pure and copper doped (2 % and 3 %) cadmium oxide grown by sol-gel is depicted in figure 3 within the wavelength range 200-2500 nm. The transmittance plot in visible spectrum, of studied samples and pure glass, is observed inset of fig.3. As can be seen the transmittance grew up rapidly in UV-VIS range until 85% for 3 % Cu doped CdO sample and continues to increase monotonically in the VIS and NIR spectra. It reaches a maximum found to be 91 %, 90 % and 89 % in IR for the 3 %, 2% Cu doped CdO and pure CdO respectively and then transmittance decreases slightly with copper doping level. Similar evolution is observed in Kumaravel paper [9, 23]. Subramanyam has found the same trend profile of transmittance in VIS and IR spectrum for the CdO films grown by DC magnetron sputtering for one particular oxygen pressure [24]. We remark that Cu ions improve considerably the optical transmittance particularly in visible range (see inset of fig.3). The average transmittance at 550 nm increases with doping level, as listed in table 1, and confirms the previous statement. We mention that low copper level doping improves the transmittance around visible edge (750-800 nm) where transmittance of 3 % Cu doped CdO approaches the pure glass transparency as can be easily seen inset of fig.3. The direct optical band gap is expressed as [4],

$$\alpha h\nu = (h\nu - E_g)^{0.5} \qquad (2)$$

Where E_g (eV) is the optical band gap, α (m^{-1}) is the absorption coefficient and ν (Hz) is the photon frequency. Band gap E_g estimates were derived from the optical transmission spectra by extrapolating the linear portion of the plot of $(\alpha h\nu)^2$ against hν to α=0 as plotted in figure 4. It varied with doping level, the pure sample exhibits E_g equals to 2.49 eV , the samples 2 % and 3 % Cu doped have respectively 2.50 and 2.56 eV as sketched in figure 4 and listed in table 1. While the optical band gap was found by T.P. Gujar is 3.18 eV [25] and Kumaravel has reported a value of E_g ~2.53 eV [23]. Others works exhibit an average of E_g around 2.46 eV [24]. Our results are in accordance with those obtained in literature [23, 24]. The estimated energy gap from $(\alpha h\nu)^2$, dT/dλ and dR/dλ (reflectance is not shown here) of pure and Cu-doped CdO films are given in Table 1. There is an effect of the Cu dopant concentrations but not regular in the studied range on the optical band gap estimated from dR/dλ versus λ (not shown here) suggesting that the optical band gap shifts from 2.49 to 2.62 eV. These gap values lead to a blue shift which may be explained by Burnstein-Moss effect. Our results are in well agreement with those of literature [6]. Fluorine has increased the band gap as reported by Akyuz [26].

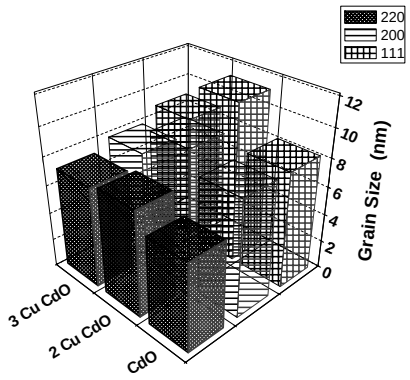

Figure 2. Grain size plot against Cu content according to (111), (200) and (220) directions

1.2. Surface morphology investigation

The 2D and 3D AFM investigation is shown in figure 5, picture have dimensions 10 x 10 micrometers. Overall, the surface of CdO coated film is homogeneous with few voids which are signed by circles as depicted in 2 D views (see fig. 5 left). Pure CdO nanograins look like mounts with no well defined boundaries; the average of grain size is 0.075 µm and height equals to 742 nm. Pure CdO coated film reveals agglomerated regions with different asperity, the bright ones (signed by arrows in fig. 5A) attract more atoms during the growth process than the dark ones which might demonstrate cavities. Similar morphology shape was reported in literature [23, 27]. 2 % Cu doped CdO sample reveals columns like wires which are separated and grown in the same direction having an average height equals to 275 nm , the 3 % Cu doped CdO shows the same shape of wires with big nanowires density (number of nanowires per μm^2) and major height (~382nm). Clusters of nanowires exhibit different sizes 0.186 µm (2 Cu % doped CdO), 0.208 µm (3 Cu % doped CdO). We conclude that low copper doping level influences the surface morphology of cadmium oxide coated film and tends to make longer the nano-grains into nanowires.

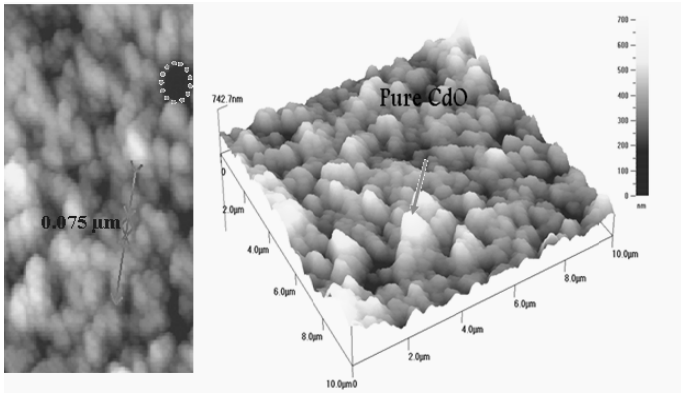

Figure 5A. AFM topography image of pure CdO coated films. AFM Pictures are 10x10 μm^2, grain size and voids are shown in (left) 2D view and (right) 3D view, (height is shown at left corner of 3D image, arrow shows nano-mounts.

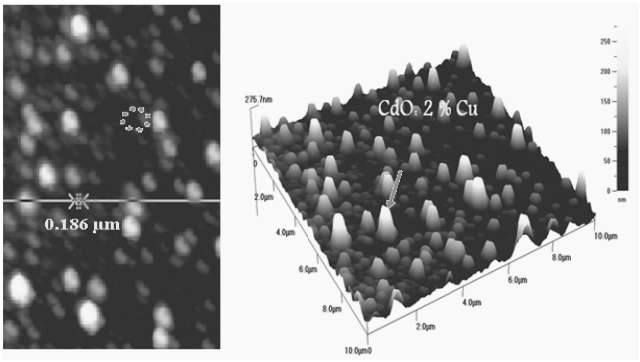

Figure 5B. AFM topography image of 2 % Cu doped CdO coated films. AFM Pictures are 10x10 µm², grain size and voids are shown in (left) 2D view and (right) 3D view, (height is shown at left corner of 3D image, arrow shows nanowires.

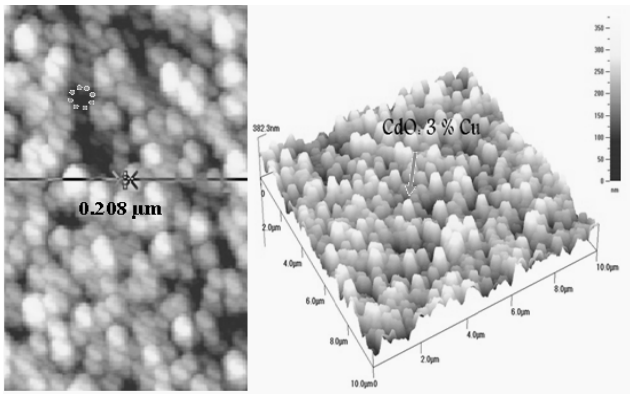

Figure 5C. AFM topography image of 3 % Cu doped CdO coated films. AFM Pictures are 10x10 µm², grain size and voids are shown in (left) 2D view and (right) 3D view, (height is shown at left corner of 3D image, arrow shows nanowires.

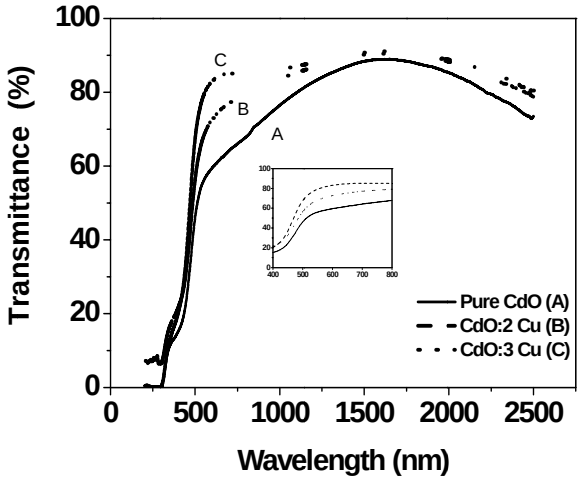

Figure 3. Transmittance dependence on photon wavelength of pure, 2 and 3% Cu doped CdO grown by spin coating at 1200 RPM, inset shows VIS transmittance profile of pure, 2 % Cu and 3% Cu doped CdO and pure glass of substrate.

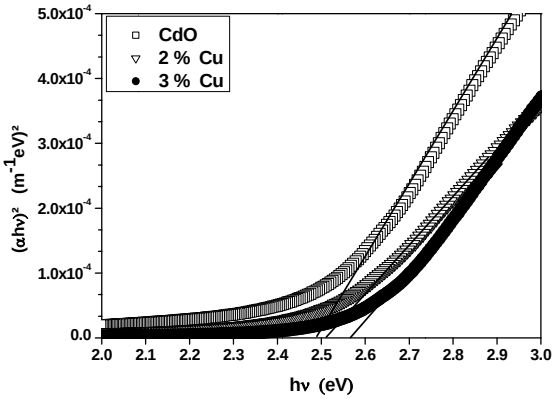

Figure 4. Dependence of $(\alpha h\nu)^2$ on incident photon energy (hν) of undoped CdO , % 2 and 3 % Cu doped CdO, (extrapolation straight lines are depicted).

1.3. Electrical measurement

The electrical measurement was carried out in four probes set up as can be seen inset of figure 6 and the electrical resistance at room temperature is depicted in figure 6. The electrical resistance R was calculated by using [28],

$$R = k\frac{V}{I} \qquad (3)$$

Where k is a constant found to be 4.53, V is the applied voltage and I is the intensity of DC current. It is observed that copper level doping diminishes greatly the resistance by about 5 and 400 times for 2 % and 3 % Cu doped CdO respectively. This fact is due to copper, which has two level of oxidation I and II, can substitute to cadmium sites and offers free electrons which can improve the conductivity.

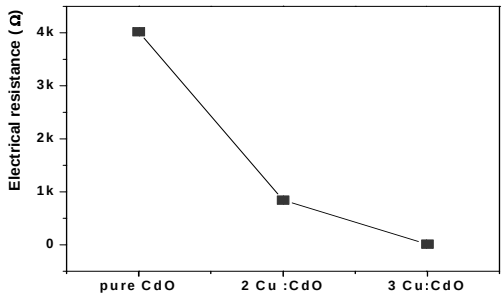

Figure 6. DC resistance at ambient is plotted versus Cu amount. Inset shows the four probes set up scheme

Conclusion

The pure and Cu doped CdO films structural, 2D and 3D AFM views, optical properties were investigated. It is revealed that CdO phase is obtained and the grain size reaches up to 11 nm according to (111) direction and TC decreases a little with copper doping level. A peak broadening reveals nanostructures formation of our coated films. High transparent coated films in VIS-IR range are obtained and low copper level doping improves the transmittance mainly in visible band edge from 56 % to 79%, and exceeds the point of 90 % in IR spectrum. Band

gap increases with copper level doping and demonstrates a blue shift. Low copper doping level maintains the crystalline structure, extends the grains and transforms them to high transparent nanowires and reduces the ambient resistance. These characteristics of high VIS-IR transparency and low resistive nanowires can provide to our coated films, produced by facile sol-gel route, various applications in material sciences and optoelectronics devices which can be investigated in next work.

Acknowledgements

This work, under contract number D 01920080054, is included in project "*CNEPRU2009-2012"* supported by the Algerian High Level Teaching and Scientific Research Ministry MESRS and Oran Sciences and Technology University USTOMB. The author would like to acknowledge the generous assistance of Pr F. Yakuphanoglu, Physics Dpt., Firat University Turkey, for his help in optical measurements, Mr. A. Avila-García, A. Tavira, Cinvestav-IPN, "Dept. Ingeniería Eléctrica", and R. R. Trujillo, "Centro de investigación en dispositivos semiconductors", Mexico for their fruitful help in performing AFM and X-rays pattern observations.

References

[1] C.E. Benouis, M. Benhaliliba, F. Yakuphanoglu, A. Tiburcio Silver , M.S. Aida, A. Sanchez Juarez, Synthetic Metals (2011). D.O.I. 10.1016/j.synthmet.2011.04.017.
[2]G. Korotcenkov , A. Cerneavschi , V. Brinzari ,A. Vasiliev , M. Ivanov, A. Cornet , J. Morante , A. Cabot , J. Arbiol, Sensors and Actuators B 99 (2004) 297-303.
[3] M.K. Fung, Y.C. Sun, A.M.C. Ng, A.B. Djurisic, W.K. Chan, Current Applied Physics 11 (2011) 594-597.
[4]M. Benhaliliba, C. E. Benouis, M. S. Aida, F. Yakuphanoglu, A. Sanchez Juarez, J. Sol-Gel Sci. Technol. 55, 3, (2010)335-342, doi 10.1007/s10971-010-2258- x.
[5]M. Benhaliliba, C.E. Benouis, M.S. Aida, A. Sanchez Juarez F. Yakuphanoglu , A. Tiburcio Silver, J. Alloys Compd. 506 (2010) 548-553.
[6] Xiaofei Han, Run Liu, Zhude Xu, Weixiang Chen, Yifan Zheng, Electrochemistry Communications 7 (2005) 1195-1198.
[7]Seval Aksoy, Yasemin Caglar, Saliha Ilican, Mujdat Caglar, International journal of hydrogen energy 34 (2009) 5191-5195.
[8] A.S. Kamble, R.C. Pawar, N.L. Tarwal, L.D. More, P.S. Patil, Materials Letters 65 (2011) 1488-1491.
[9]R. Kumaravel, K.Ramamurthi, Indra Sulania, K.Asokan, D.Kanjilal, D.K.Avasti, P.K.Kulria, Radiation Physics and Chemistry 80 (2011) 435-439.
[10]Qiang Zhou, Zhenguo Ji, BinBin Hu, Chen Chen, Lina Zhao, Chao Wang, Materials Letters 61 (2007) 531-534.
[11] H.B. Lu, L. Liao, H. Li, Y. Tian, D.F. Wang, J.C. Li, Q. Fu, B.P. Zhu , Y. Wu, Materials Letters 62 (2008) 3928-3930.
[12]A. Gulino, G. Tabbi, Appl. Surf. Sci. 245 (2005), 322-327.
[13]A.A. Dakhel, Effect of thermal annealing in different gas atmospheres on the structural, optical, and electrical properties of Li-doped CdO nanocrystalline films, Solid State Sciences (2011), doi:10.1016/j.solidstatesciences.2011.02.002.
[14]K.R. Murali, A. Kalaivanan, S. Perumal, N. Neelakanda Pillai, Journal of Alloys and Compounds 503 (2010) 350-353.
[15] A.A. Dakhel, Thin Solid Films 518 (2010) 1712-1715.
[16] A.A. Dakhel, Solar Energy 82 (2008) 513-519.
[17]A.A. Dakhel, Journal of Alloys and Compounds 475 (2009) 51-54.
[18]A.A. Dakhel, Current Applied Physics 11 (2011) 11-15.
[19]A.A. Dakhel, Optical Materials 31 (2009) 691-695.
[20]Robert Corriu, Nguyen Trong Anh, molecular chemistry of Sol-gel derived nanomaterials, Wiley Ed. ISBN 978-0-470-72117-9 (2009).
[21]Salih Kose, Ferhunde Atay, Vildan Bilgin, Idris Akyuz, International Journal of Hydrogen Energy 34 (2009) 5260-5266.
[22]A.A. Dakhel, Materials Chemistry and Physics117 (2009)284-287.
[23]R. Kumaravel, S. Menaka, S. Regina Mary Snega, K. Ramamurthi, K. Jeganathan, Materials Chemistry and Physics 122 (2010) 444-448.
[24] T.K. Subramanyam, S. Uthanna, B. Srinivasulu Naidu, Materials Letters 35, (1998), 214-220.
[25]T.P. Gujar, V.R. Shinde, Woo-Young Kim, Kwang-Deog Jung, C.D. Lokhande, Oh-Shim Joo, Applied Surface Science 254 (2008) 3813-3818.
[26]I. Akyuz, S. Kose, E. Ketenci, V. Bilgin, F. Atay, Journal of Alloys and Compounds 509 (2011) 1947-1952.
[27]D.M. Carballeda-Galicia, R. Castanedo-Pérez, O. Jiménez-Sandoval, S. Jiménez-Sandoval, G. Torres-Delgado, C.I. Zuniga-Romero, Thin Solid Films 371, (2000) 105-108.
[28]R. Legros, les semiconducteurs, Vol.1, Eyrolles Ed. (1974).